Published OnlineFirst November 26, 2018; DOI: 10.1158/0008-5472.CAN-18-2488

Tumor Biology and Immunology

Cancer Research

Stathmin Is Required for Normal Mouse Mammary Gland Development and Δ16HER2-Driven Tumorigenesis

Ilenia Segatto[1], Mara De Marco Zompit[1], Francesca Citron[1], Sara D'Andrea[1], Gian Luca Rampioni Vinciguerra[1,2], Tiziana Perin[3], Stefania Berton[1], Giorgia Mungo[1], Monica Schiappacassi[1], Cristina Marchini[4], Augusto Amici[4], Andrea Vecchione[2], Gustavo Baldassarre[1], and Barbara Belletti[1]

Abstract

Postnatal development of the mammary gland relies on the maintenance of oriented cell division and apicobasal polarity, both of which are often deregulated in cancer. The microtubule (MT) network contributes to control these processes; however, very little is known about the impact of altered MT dynamics in the development of a complex organ and on the role played by MT-interacting proteins such as stathmin. In this study, we report that female stathmin knockout (STM KO) mice are unable to nurse their litters due to frank impairment of mammary gland development. In mouse mammary epithelial cells, loss of stathmin compromised the trafficking of polarized proteins and the achievement of proper apicobasal polarity. In particular, prolactin receptor internalization and localization was altered in STM KO mammary epithelial cells, leading to decreased protein stability and downmodulation of the Prl/PrlR/STAT5 signaling pathway. Absence of stathmin induced alterations in mitotic spindle orientation, accumulation of mitotic defects, and apoptosis, overall contributing to tissue disorganization and further decreasing the expansion of the mammary epithelial compartment. Loss of stathmin in MMTV-Δ16HER2 transgenic mice decreased the incidence and increased the latency of these very aggressive mammary carcinomas. Collectively, these data identify the essential mammary protein stathmin as protumorigenic and suggest it may serve as a potential therapeutic target in breast cancer.

Significance: Stathmin expression is critical to maintain oriented cell division and apicobasal polarity in normal mammary glands and to establish a protumorigenic program that eventually sustains HER2-positive breast cancer formation in mice.

Introduction

The mammary gland is a highly dynamic and adaptive organ that completes its morphologic development postnatally, during puberty and pregnancy (1). The integrity of the mammary gland relies on the maintenance of oriented cell division and apicobasal polarity and the preservation of these characteristics is essential not only for mammary gland functionality, mainly during lactation, but also for preventing breast cancer. Accordingly, the study of the mammary gland normal development represents an excellent model for studying the mechanisms underlying tumorigenesis (1, 2).

Stathmin 1 (hereafter stathmin) is a microtubule (MT)-destabilizing protein and, as such, it is critically involved in the regulation of mitosis, vesicular trafficking, and cell motility. At the onset of mitosis, stathmin is phosphorylated by Aurora B kinase and cyclin-dependent kinases, to allow for correct formation of mitotic spindle (3). At the end of mitosis, the mitotic spindle is disassembled and stathmin activity is turned on by dephosphorylation events, eventually triggering the microtubule catastrophe and the correct division of the two daughter cells. Achievement of a balance between MT-stabilizing and -destabilizing activities in the cell is critical to properly orient the mitotic spindle and avoid mitotic aberrations (4).

During interphase, MTs are implicated in the maintenance of the epithelial polarity, because MT orientation along the apicobasal axis directs intracellular trafficking and MTs serves as tracks for cargos, such as organelles and vesicles (5). Accordingly, the inhibition of MT-dependent transport by taxol, dynamin, or dynein inhibitors impairs the full activation of intracellular signaling cascades, such as the Ras/MAPK pathway. Stathmin is involved in this process and its activity needs to be finely tuned for proper Ras recycling and activation (6).

Although dispensable for mouse tumor onset during chemical carcinogenesis of the muscle, bladder, and skin (7), stathmin is

[1]Unit of Molecular Oncology, Centro di Riferimento Oncologico di Aviano (CRO), IRCCS, National Cancer Institute, Aviano, Italy. [2]Faculty of Medicine and Psychology, Department of Clinical and Molecular Medicine, University of Rome "Sapienza" Sant'Andrea Hospital, Rome, Italy. [3]Unit of Pathology, Centro di Riferimento Oncologico di Aviano (CRO), IRCCS, National Cancer Institute, Aviano, Italy. [4]Department of Biosciences and Veterinary Medicine, University of Camerino, Camerino, Italy.

Note: Supplementary data for this article are available at Cancer Research Online (http://cancerres.aacrjournals.org/).

G. Baldassarre and B. Belletti contributed equally to this article.

Corresponding Authors: Gustavo Baldassarre, Centro di Riferimento Oncologico di Aviano (CRO), IRCCS National Cancer Institute, Via F. Gallini 2, 33081 Aviano, Italy. Phone: 39-0434-659-759; E-mail: gbaldassarre@cro.it; and Barbara Belletti, Centro di Riferimento Oncologico di Aviano (CRO), IRCCS National Cancer Institute, Via F. Gallini 2, 33081 Aviano, Italy. Phone: 39-0434-659-661; E-mail: bbelletti@cro.it

doi: 10.1158/0008-5472.CAN-18-2488

Published OnlineFirst November 26, 2018; DOI: 10.1158/0008-5472.CAN-18-2488

highly expressed in several types of human tumors, including breast cancer, and its high expression correlates with more malignant behavior of the tumor and poor prognosis of the patients (8, 9).

Stathmin role during mammary gland maturation and breast cancer onset has never been investigated, so far. Here, by breeding and characterizing stathmin knock-out female mice, we have investigated the role of stathmin during mammary gland development and, by intercrossing them with the Δ16HER2 transgenic mice, we have explored its involvement in mammary tumorigenesis. The Δ16HER2 is a splice variant of HER2 lacking exon 16 that has been frequently detected in human breast carcinomas. When expressed in the MMTV-Δ16HER2 transgenic mouse model, Δ16HER2 displays a greatly enhanced transforming activity compared with wild-type HER2 (10).

Here, by investigating the role of stathmin during mammary morphogenesis, we discover that stathmin expression is necessary for both normal mammary gland postnatal development and for Δ16HER2-driven tumor onset.

Materials and Methods

Study approval

Animal experimentation was approved by the Italian Ministry of Health (#616/2015-PR) and by our Institutional Animal Care and Use Committee (OPBA). *In vivo* experimentation was conducted strictly complying with OPBA and internationally accepted Institutional Animal Care and Use Committee guidelines for animal research and with the 3R principles.

Animal experimentation and *ex vivo* analyses

FVB stathmin knock-out mice (STM KO) were housed and bred as described previously (7). MMTV-Δ16HER2 mice were generated and previously characterized (10) and were housed in our animal facility. Detailed protocols can be found in Supplementary Information.

Apoptosis and immunofluorescence

Detection of apoptosis was performed by TUNEL assay, using In Situ Cell Death Detection Kit, AP (Roche) or by propidium iodide uptake in live culture (11). Immunofluorescence analyses were performed on cultured cells and mammary acini grown in 3D cultures, as described previously (11–14). Detailed protocols can be found in Supplementary Information.

Mitotic spindle orientation measurements

In mammary glands and in cells grown in 3D matrix, the mitotic spindle orientation was measured in sections stained for pSer10 Histone H3 (pSer10-H3), α-tubulin, and nuclei, as reported by others (15–17). Detailed protocols can be found in Supplementary Information.

Cell culture, qRT-PCR, and Western Blot analyses

BPE-3 cells were purchased from Live Tissue Culture Service Center (LTCC; LTCC@med.miami.edu) and grown in BMI-P medium (LTCC), supplemented with cholera toxin 100 ng/mL (Sigma), as published previously (18) and strictly following all manufacturer's instructions. NMuMG cells were a kind gift of Dr. Andrei V. Bakin at Roswell Park Comprehensive Cancer Center (Buffalo, NY; ref. 19) and grown in DMEM (Sigma) and supplemented with 10% FBS (Carlo Erba). BPE-3 and NMuMG cells were expanded and frozen immediately into numerous aliquots immediately after their arrival. Cells revived from the frozen stock were then used for 4 to 6 passages and, however, not exceeding a period of 1 month. HEK293 cells (ATCC) and 293FT cells (Invitrogen, Thermo Fisher Scientific) were used for adenoviral or lentiviral production and grown in DMEM supplemented with 10% FBS (Carlo Erba). All cell lines were routinely tested to exclude *Mycoplasma* contamination (MycoAlert, Lonza). Human cell lines were authenticated by short tandem repeat (STR) analysis in 2018, according to PowerPlex 16 HS System (Promega) protocol and using GeneMapper software 5 (Thermo Fisher Scientific) to identify DNA STR profiles. Stathmin-silenced cells were generated by adenoviral or lentiviral system, as indicated. The adenoviral system used to silence stathmin expression has been described elsewhere (20, 21). RNA from mammary tissue or cells was extracted using TRIzol reagent (Invitrogen). Protein lysates and Western blot analyses were performed essentially as described previously (22). Detailed protocols can be found in Supplementary Information.

Time-lapse microscopy

To evaluate mitosis duration and mitotic defects associated with cell death, stathmin-silenced or control NMuMG clones were seeded in 12-well plate (7.5×10^4 cells/well) and video-recorded for 16 hours at 37°C with controlled humidity and CO_2 concentration, using timelapse AF6000LX workstation (Leica). Images were collected every 5 minutes, using a 20× objective. Video was generated assembling the images with the Volocity software (PerkinElmer), as described previously (6, 23).

Colony and soft-agar assay

NMuMG Δ16HER2–expressing cells, silenced or not for stathmin, were seeded and incubated in complete medium. After 2 weeks, crystal violet–stained colonies or soft-agar colonies were manually counted, as described previously (12, 24). Detailed protocols can be found in Supplementary Information.

Gene expression profiling and data mining tools

Gene expression profiling (GEP) were performed essentially as described previously (25). Briefly, RNA from mammary glands of 13 weeks old Δ16HER2-WT and -STM KO mice was extracted using TRIzol and purified in columns of RNEasy kit (Qiagen). GEP was performed with 150 ng total RNA labeled with cyanine (Cy)-3 dye. Cy3-labeled RNA was hybridized to the Whole Mouse Genome (4 × 44 K) oligo microarray (Agilent Technologies) and analyzed with an Agilent Microarray Scanner (Agilent Technologies) and with the Agilent Feature Extraction Software 10.7.3 (Agilent Technologies), as reported previously (25). After preprocessing and prefiltering steps, the final dataset was subjected to supervised analyses using GeneSpring (Agilent Technologies). Gene expression profile results were visualized by hierarchical clustering applying Ward's method with Euclidean distance. Microarray data have been deposited in NCBI Gene Expression Omnibus (GEO) repository (#GSE121088).

Statistical analyses

Statistical significance, means, median, and SD were determined by using GraphPad PRISM software (version 6.01), using the most appropriate test, as specified in each figure. Significance is indicated by a $P < 0.05$. More details on the statistical methods can be found in Supplementary Information.

Published OnlineFirst November 26, 2018; DOI: 10.1158/0008-5472.CAN-18-2488

Results

Stathmin KO female mice display severe lactation defects

Stathmin (STM) KO mice are viable and do not exhibit overt developmental abnormalities, as previously reported by our group and others (25, 26). However, we observed that litter born from STM KO female mice very frequently died one-day postpartum (Fig. 1A). This phenotype was not strain dependent (Supplementary Fig. S1A) and was mitigated after the second pregnancy, when the number of viable litters born from STM KO mice reached approximately 50% (Fig. 1A, graph). No macroscopic morphologic defects were observed in pups born from STM KO mice, but examination of their stomach showed that no milk was present, suggesting that STM KO females failed to nurse (Fig. 1A, pictures).

On the basis of this phenotype, we decided to study in more detail the morphology of murine mammary glands (MMG) in WT and STM KO mice. We collected the inguinal MMG from prepubertal (5 weeks of age), adult virgin (9–11 weeks of age), day 13.5 of pregnancy, and one-day postpartum (lactation) female mice. At all stages analyzed, but in particular during pregnancy and lactation, STM KO mice exhibited a delay in mammary development, displaying lower number of branches and side ramifications (Fig. 1B). In WT animals, alveolar structures of lactating MMG were clearly turned into milk-secreting lobules covering the entire mammary fat pad, while in STM KO mice, they were still immature and displayed abundant adipose tissue in the interductal spaces (Fig. 1B, bottom) with the area covered by epithelial mammary structures significantly reduced (Fig. 1C; Supplementary Fig. S1B). In accord with these results, during pregnancy and lactation, stathmin RNA and protein expression strongly increased in WT MMG (Fig. 1D and E) and other stathmin family members did not compensate for stathmin loss in STM KO MMG (Supplementary Fig. S1C).

Together, these results suggest that stathmin plays a critical role in normal MMG postnatal development.

Loss of stathmin reduces the proliferative rate of mammary epithelial cells

We next determined whether loss of stathmin affected the proliferation and/or apoptosis of mammary epithelial cells. At all stages analyzed, STM KO MMG showed a decreased proliferation rate in comparison with WT ones (Fig. 2A; Supplementary Fig. S2A) and an increase in apoptosis (Fig. 2B; Supplementary Fig. S2B). These results were also confirmed *in vitro*, using mouse

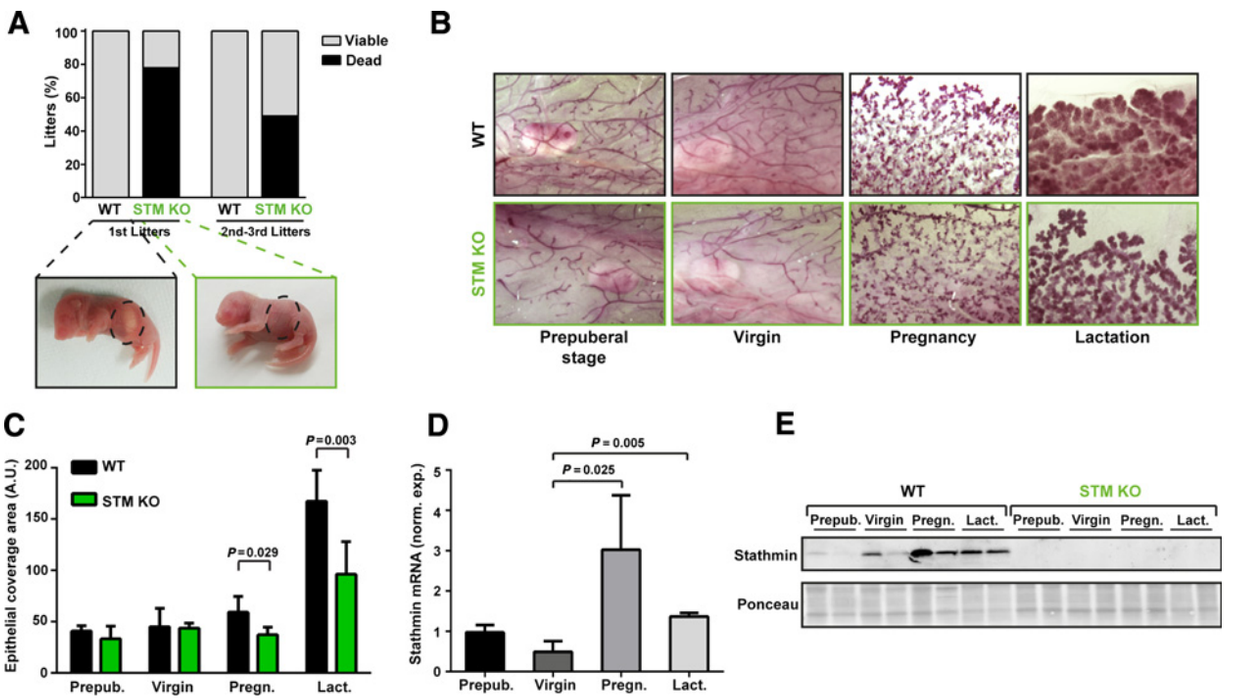

Figure 1.

Loss of stathmin impairs mouse mammary gland development. **A,** Graph reports the percentage of viable litters born from WT or STM KO female mice in the first or following pregnancies, as indicated. Litters were considered viable when at least one pup was nursed and survived. Bottom, representative pictures of pups born from WT (left) or STM KO (right) dam are reported. Dashed line highlights the pup stomach, with or without milk inside. Data from C57/BL6 and FVB mouse backgrounds were merged together and at least 25 litters/genotype were evaluated. **B,** Whole mount of mammary glands collected from WT (top) and STM KO (bottom) female mice at different phases of development: prepubertal stage (5 weeks of age), adult virgin (9–11 weeks of age), during pregnancy (day 13.5 of gestation), and during lactation (one day postpartum). At least four mice/stage/genotype were analyzed. **C,** Quantification of epithelial coverage per area (ducts and alveoli) in hematoxylin and eosin–stained mammary gland sections (shown in Supplementary Fig. S1A), collected at the same developmental stages described in **B**. Images were taken with a 5× objective and quantified with the ImageJ software. **D,** qRT-PCR analysis of stathmin transcript level in WT mammary glands, collected at the indicated stages. **E,** Representative Western blot analysis of stathmin protein level in lysates from WT and KO mammary glands, collected at the indicated stages. Ponceau staining was used as loading control. From **B** to **E**, results are from $n = 4$ samples/stage. In all graphs, significance was calculated by Student t test and is indicated by a $P < 0.05$.

Published OnlineFirst November 26, 2018; DOI: 10.1158/0008-5472.CAN-18-2488

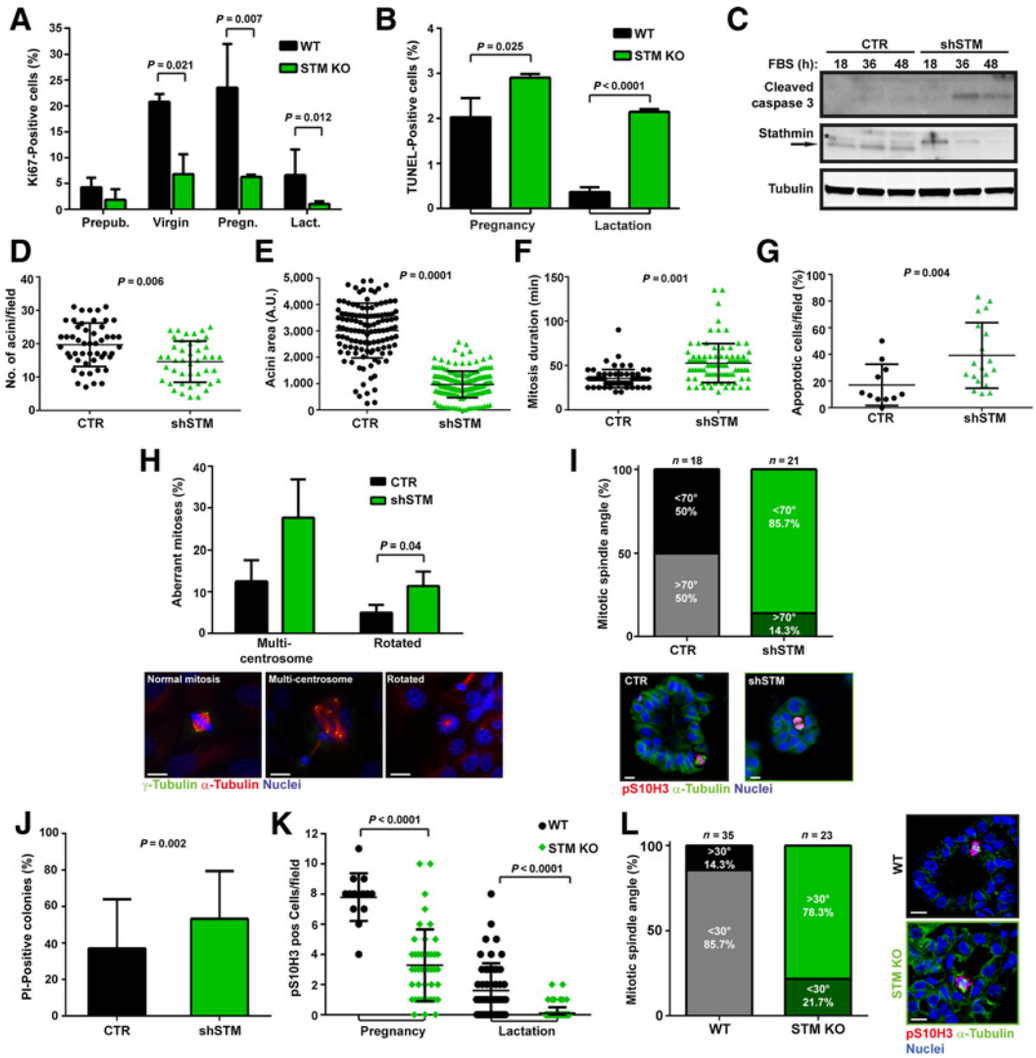

Figure 2.

Loss of stathmin decreases proliferation and alters mitotic spindle orientation of mammary epithelial cells. **A,** Graph reports the percentage of Ki67-positive cells, evaluated by IF, in mammary glands from WT and STM KO female mice, collected at the indicated stages. **B,** Histogram displays the percentage of apoptotic cells, evaluated by TUNEL assay, in mammary tissue collected from WT and STM KO mice during pregnancy and lactation. In **A** and **B**, results are from $n = 4$ samples/stage/genotype. At least 10 fields/section from 63× pictures were scored. **C,** Immunoblot analysis of indicated proteins in NMuMG cells transduced with adenoviral particles expressing shCTR or shSTM, serum starved and released in complete medium for the indicated times. Tubulin was used as loading control. Arrow, specific stathmin band. Asterisk, nonspecific band. **D,** Acini formation assay in 3D Matrigel of human breast primary epithelial cells (BPE-3) silenced for stathmin (shSTM) or not (CTR). Ten days after Matrigel embedding, the number of colonies/field was counted. **E,** Colony area of experiment described in **D** measured using the Volocity software and expressed in arbitrary units (A.U.). Each dot corresponds to one colony. **F** and **G,** Graphs report the duration of mitosis (**F**) and the number of cells unable to successfully resolve mitosis and dying over the total number of mitoses/field (**G**) evaluated by time-lapse microscopy in CTR and shSTM NMuMG, serum starved, and released in complete medium and recorded every 5 minutes for 16 hours. For calculating the duration of mitosis, at least 30 mitotic events/clone were measured. Three different silenced clones were tested in both experiments. **H,** Graph (top) and representative images (bottom) reporting the percentage of aberrant mitoses in CTR and shSTM NMuMG, serum starved, released for 18 hours in complete medium, and analyzed by immunofluorescence. Multi-centrosome or mitoses with altered mitotic spindle orientation (rotated) were counted in three different clones. Cells were immunostained with γ-tubulin (green), α-tubulin (red), and nuclei (TO-PRO-3, blue). Scale bars, 11 μm. **I,** Graph (top) and representative images (bottom) reporting the percentage of cells showing a mitotic spindle angle higher or lower than 70°, evaluated in CTR and shSTM BPE-3 cells, grown in 3D Matrigel. The angle was calculated measuring the intersection of a line drawn between the spindle poles (spindle axis) and a line drawn from the acini centroid to the midpoint of the spindle axis. The 3D acini were immunostained for pSer10-H3 (red), α-tubulin (green), and nuclei (TO-PRO-3, blue). Confocal images of metaphase or anaphase mitotic cells were collected and analyzed using the ImageJ software. Scale bars, 11 μm. **J,** Graph reports the quantification of 3D colonies presenting NMuMG cells (control and shSTM, as indicated) uptaking the propidium iodide in live culture. Values indicate the percentage of positive colonies over the number of total colonies. **K,** Graph reports the quantification of mitotic cells/field in WT and STM KO mammary glands collected during pregnancy and lactation. Sections were stained for pSer10-H3 and positive cells were counted from 63× images. Results are from $n = 4$ samples/stage. At least 10 fields/section were scored and counted. **L,** Left, graph reports the percentage of cells showing a mitotic spindle angle higher or lower than 30°, evaluated in mammary gland sections from WT and STM KO mice during lactation. The angle was calculated measuring the intersection between the spindle axis of mitotic cells and the basement membrane. Right, representative images show the immunostaining for pSer10-H3 (red), α-tubulin (green), and nuclei (TO-PRO-3, blue). Scale bars, 10 μm. When not otherwise specified, $n = 3$ independent experiments were conducted. In all graphs, significance was calculated by Student t test or Mann–Whitney test, as appropriate, and is indicated by a $P < 0.05$.

Published OnlineFirst November 26, 2018; DOI: 10.1158/0008-5472.CAN-18-2488

and human normal mammary epithelial cells (NMuMG and BPE-3; ref. 18), silenced for stathmin (shSTM) or not (control, CTR). When challenged with serum starvation and release, stathmin-silenced cells displayed a pronounced upregulation of apoptotic markers, as measured by cleaved caspase-3 levels (Fig. 2C). When grown in 3D Matrigel, both number and area of the mammary acini reflected what observed *in vivo* and loss of stathmin led to a significant decrease in the ability to form colonies (Fig. 2D and E, for BPE-3 cells; Supplementary Fig. S2C-S2F, for NMuMG cells).

These data suggest that stathmin is important for achieving the right level of proliferation and survival in the mouse mammary epithelial cell compartment, particularly during those developmental stages, such as pregnancy and lactation, in which great expansion is needed.

Stathmin controls mitotic duration and spindle orientation in dividing mouse mammary epithelial cells

Stathmin expression and function is necessary for the completion of a successful mitosis, both in normal and tumor-derived cells (21, 27). Maintenance of proper cell division is fundamental for preserving correct polarity in the mammary epithelial compartment (15, 28, 29). We thus analyzed by time-lapse microscopy the progression through the cell cycle of NMuMG cells in culture. shSTM cells showed a significant delay in the time required to progress from cell round-up to cytokinesis and, as a consequence, the duration of their mitosis almost doubled the one of CTR cells (Fig. 2F). When counting cells that were unable to successfully resolve the mitosis, we could appreciate that stathmin-silenced cells died significantly more than control cells and were continuously cleared out from the culture (Fig. 2G; Supplementary Video S1 and S2).

Thus, we more carefully investigated the mitoses of proliferating shSTM cells and noted that the outcome was often aberrant. In 2D culture, where the mitotic spindle orientation is roughly parallel to the substrate plane (30), we observed an increased number of cells displaying misaligned spindle and/or multi-centrosomes when stathmin was silenced (Fig. 2H). In 3D culture, where orientation of the spindle is critical for the formation of correctly polarized mammary acini (16, 17), we observed that in control acini the majority of spindles were, as expected, oriented perpendicular to the lumen (i.e., angle $\geq 70°$), whereas in stathmin-depleted cells, spindle orientation was randomized and the percentage of spindle oriented perpendicular to the lumen was reduced to 14% (Fig. 2I). As a consequence, the acini formed by stathmin-silenced cells displayed significantly higher apoptotic rate than those of control cells (Fig. 2J).

Importantly, the same findings were recapitulated in the mammary gland, *in vivo*. Significantly fewer cells were positive for the mitotic marker pSer10-Histone H3 in STM KO MMG (Fig. 2K). As expected, 86% of the mitotic cells in normal mammary glands displayed their spindles oriented parallel to the basement membrane (angle 0°–30°; ref. 15), whereas only 22% of STM KO mitotic cells fell into this category and the majority exhibited abnormal spindle orientation with an angle $\geq 30°$ (Fig. 2L).

These data indicate that loss of stathmin in mouse mammary epithelial cells results in alteration of spindle orientation, in mitotic aberration and delayed mitosis completion, which together possibly lead to increased cell death and, eventually, reduced mammary cell expansion.

STM KO mammary glands display a disordered organization

An altered mitotic division is likely to impact on the architecture of the whole mammary gland (31). Accordingly, while in WT MMG, we observed the typical organization of the mammary epithelium, with ductal structures composed by an outer layer of myoepithelial cells (cytokeratin 14, in green) and an inner layer of luminal cells (cytokeratin 8, in red) that delineate the lumen, at all stages of development (Fig. 3A, for the lactation stage, and Supplementary Fig. S3, for all other stages), MMG collected from STM KO mice displayed poorly organized structures, in which bilayered ducts were hardly detectable and occasionally filled with both luminal and myoepithelial cells (Supplementary Fig. S3). This phenotype was exacerbated in STM KO mammary glands collected one-day postpartum, in which, although some ductal and alveolar structures were present, their organization was largely immature compared with the WT counterpart (Fig. 3A). In addition, when we looked at proteins that typically localize with an apicobasal polarity, such as WAP, E-cadherin and Rab7, we observed that the well-ordered asset of these markers was profoundly altered in STM KO MMG (Fig. 3A).

To understand whether these alterations were due to defects intrinsic to the mammary epithelial cells or whether the stromal counterpart contributed to it, we isolated mouse primary mammary epithelial cells (mMEC) from the MMG and challenged them to form organotypic cultures in 3D Matrigel. Consistent with what observed *in vivo*, also in this context STM KO mMECs formed smaller and disorganized acinar structures (Fig. 3B).

Overall, these data suggest that loss of stathmin expression in mammary epithelial cells leads to severe defects in MMG organization and development, through a cell-autonomous mechanism.

Loss of stathmin alters the Prl/PrlR/STAT5 signaling pathway

A major driver of mammary development during pregnancy and lactation is the pituitary hormone prolactin (Prl). Intriguingly, female mice carrying in heterozygosis a germline mutation of the prolactin receptor gene (Prlr) showed a substantially overlapping phenotype to what we observed in the STM KO model, resulting in failure of lactation due to reduced mammary gland development after their first, but less in subsequent, pregnancies (32, 33).

We thus evaluated the status of Prl/PrlR signaling pathway in our setting. No significant change was detected in prolactin levels between WT and STM KO mice, either in MMG lysates or in serum (Fig. 4A). However, PrlR protein was significantly decreased in STM KO versus WT MMG, while the mRNA levels remained comparable (Fig. 4B and C). Despite some variability in Western blot analysis, mainly due to mammary fat tissue contamination, the level of activation of PrlR downstream signal transducer, STAT5, was consistently and robustly decreased in all STM KO mammary glands (Fig. 4C and D). Accordingly, also expression of milk proteins, representing transcriptional targets of STAT5, such as α- and β-casein and WAP, was decreased (Fig. 4E). These data were also confirmed in WT and STM KO mMECs and in CTR and shSTM NMuMG cells stimulated *in vitro* with prolactin (Fig. 4F; Supplementary Fig. S4A–S4C), overall demonstrating a deficient activation of the Prl/PrlR/STAT5 signaling pathway when stathmin expression was lost.

Loss of stathmin alters PrlR stability

Given that stathmin expression is critical for apicobasal polarity (above results) and is also involved in vesicle trafficking and

Published OnlineFirst November 26, 2018; DOI: 10.1158/0008-5472.CAN-18-2488

recycling of proteins (6), we hypothesized that it could impact on PrlR signaling by altering its localization and/or stability. We thus looked at PrlR levels in CTR- or shSTM NMuMG cells stimulated with Prl. Blocking protein neosynthesis, we observed that PrlR stability quickly dropped down in shSTM-cells while, in the same time frame, it remained quite stable in CTR ones (Fig. 5A). In the same cells, PrlR expression and localization was monitored by immunofluorescence over the time. Already after 5 minutes from Prl stimulation, CTR cells started to internalize the receptor and a substantial fraction of it recycled to the cell membrane within 1 hour. Conversely, shSTM cells displayed delayed internalization coupled with no recycling of the receptor to the plasma membrane (Fig. 5B). To confirm these results, we treated NMuMG cells with the microtubule-stabilizing drug Taxol, at a dose known to specifically target MT dynamics without interfering with cell proliferation and survival (5, 6, 29). We similarly observed a decrease in PrlR expression (Fig. 5C), further suggesting that proper MT dynamics and, thus, balanced expression and activity of stathmin are required for PrlR recycling and activation of the Prl pathway.

Altogether, these data provide evidence that stathmin loss in the mammary epithelium induces an altered PrlR trafficking and stability, eventually leading to Prl/PrlR/STAT5 pathway down modulation.

High stathmin expression correlates with poor prognosis in patients with breast cancer

Perturbation of the mechanisms governing cell proliferation and differentiation in the normal mammary gland are strongly implicated in breast cancer development (2). Stathmin overexpression has been detected in several cancer types (8, 34). In breast cancer, high stathmin expression positively correlates with high proliferation rate, aggressiveness, and it has been proposed as potential predictor of poor outcome (8, 9, 34). Using the Kaplan–Meier Plotter online tool (http://kmplot.com) to analyze patients with breast cancer ($n = 3{,}951$), we generated a Kaplan–Meier survival curve based on stathmin mRNA expression. The resulting curve confirmed the literature data, showing that higher expression of stathmin correlated with shorter disease-free survival of patients with breast cancer, both when putting all patients with

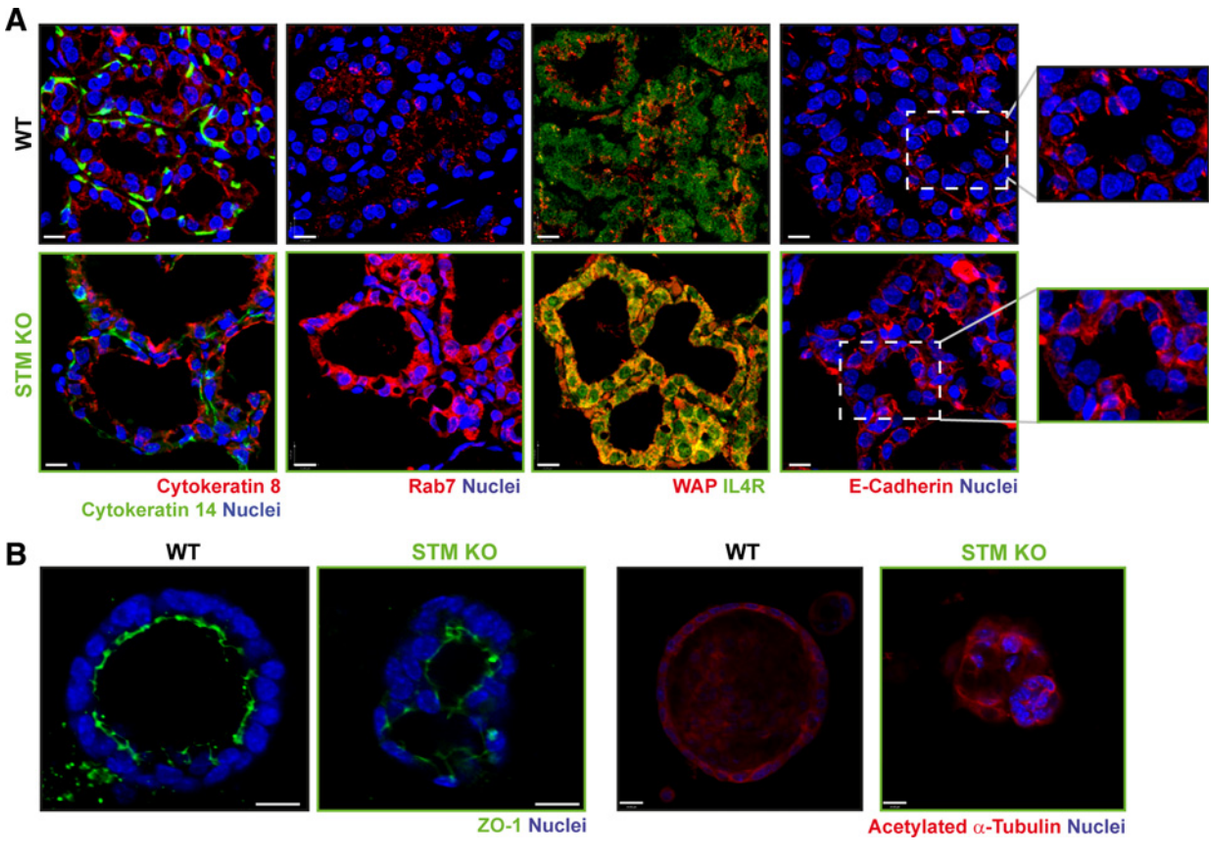

Figure 3.

Loss of stathmin alters the mammary gland organization. **A,** Representative images of immunofluorescence analyses of mouse mammary glands collected from WT or STM KO mice during lactation, as indicated. At least three MMG/genotype were analyzed. Tissue sections were immunostained (from left to right) for cytokeratin 8 (luminal marker, red), cytokeratin 14 (basal marker, green), and nuclei (TO-PRO-3, blue); Rab7 (red) and nuclei (TO-PRO-3, blue); IL4R (green) and whey acidic protein (WAP; red); E-cadherin (red) and nuclei (TO-PRO-3, blue), as indicated. On the right side, an enlargement of the E-cadherin/nuclei panels, to highlight differences in the duct structure, is shown. Scale bars, 11 μm. **B,** Acini formation assay in 3D Matrigel of primary mMECs extracted from WT and STM KO mammary glands ($n = 3$). Twelve days after Matrigel embedding, the colonies were immunostained for ZO-1 (green) and nuclei (TO-PRO-3, blue; left), and for acetylated α-tubulin (red) and nuclei (TO-PRO-3, blue; right). Scale bars, 14 μm.

Published OnlineFirst November 26, 2018; DOI: 10.1158/0008-5472.CAN-18-2488

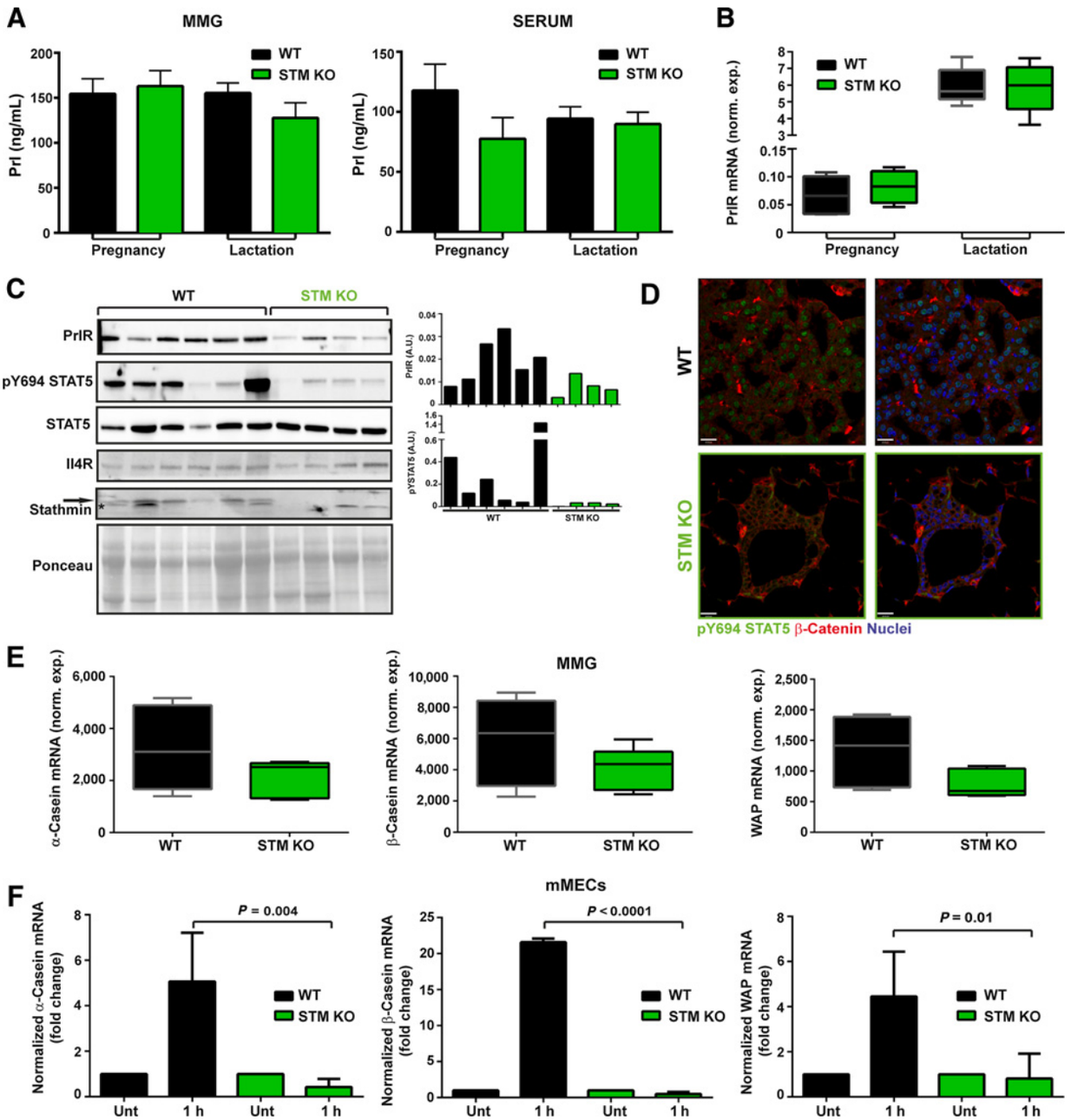

Figure 4.

Loss of stathmin leads to decreased STAT5 activation. **A,** Graph reports the results from ELISA assay evaluating the concentration of prolactin hormone in mouse MMG lysates (left) and in circulation (serum; right), in WT and STM KO mice during pregnancy and lactation, as indicated. **B,** Graph reports the normalized transcript level of PrlR in MMG collected from WT and STM KO mice during pregnancy and lactation, as indicated. At least four mice/genotype were analyzed. **C,** Western blot analysis of protein lysates extracted from MMG of WT and STM KO mice during lactation, as indicated. Each lane corresponds to a different mouse. Ponceau staining was used as loading control. Arrow, specific stathmin band. Asterisk, a nonspecific band. Right, graphs report the quantification of the bands corresponding to pY694 STAT5 and PrlR, normalized by the total level of STAT5 and by the Ponceau staining of the lysates. **D,** Immunofluorescence analysis of pY694 STAT5 (green), β-catenin (red), and nuclei (TO-PRO-3, blue), performed on sections of MMG collected from WT and STM KO mice during lactation. Scale bars, 18 μm. **E,** qRT-PCR analysis of STAT5 target genes in MMG collected from WT and STM KO mice during lactation. Normalized mRNA level of α-Casein, β-casein, and WAP is reported. At least four mice/genotype were analyzed. **F,** qRT-PCR analysis of STAT5 target genes, α-Casein, β-Casein, and WAP in mouse primary mMECs extracted from WT and STM KO virgin mice, serum starved (untreated, Unt), and stimulated with murine prolactin (100 ng/mL) for 1 hour. Results derive from the use of $n = 3$ cell populations/genotype and are expressed as fold change in respect to the untreated. When box whisker plots were used, minimum, median, and maximum values are shown in the graph. In all graphs, significance was calculated by Student *t* test or Mann–Whitney test, as appropriate, and is indicated by a $P < 0.05$.

Published OnlineFirst November 26, 2018; DOI: 10.1158/0008-5472.CAN-18-2488

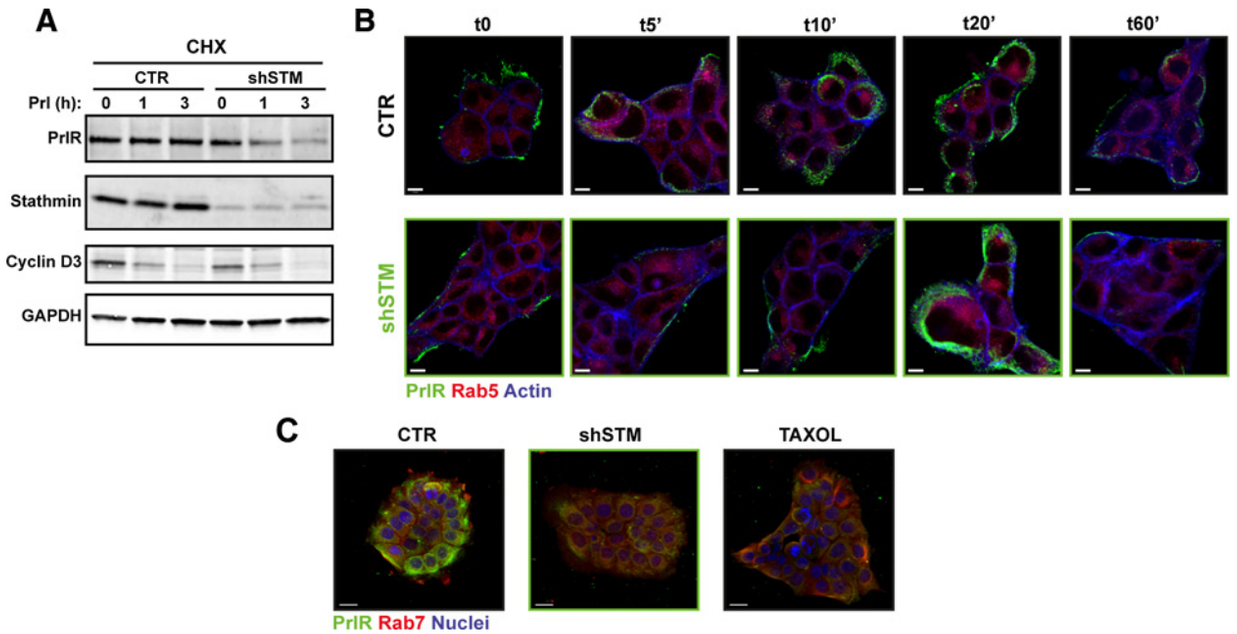

Figure 5.

Stathmin modulates PrlR stability. **A,** Western blot analysis of PrlR in NMuMG control cells (CTR) or silenced for stathmin (shSTM). Cells were serum starved overnight, treated with cycloheximide (CHX; 50 μg/mL) for 2 hours and then stimulated with murine Prl (200 ng/mL) for indicated times. GAPDH was used as loading control. **B,** Analysis of PrlR internalization and trafficking in NMuMG cells control cells (CTR) or silenced for stathmin (shSTM). Cells were serum starved for 4 hours and stimulated with murine Prl (100 ng/mL) for 1 hour on ice. Cells were then incubated at 37°C for the indicated time and immunostained with PrlR (green), RAB5 (red), and phalloidin (blue). Scale bars, 7 μm. **C,** Representative confocal images of NMuMG CTR cells, STM-silenced cells (shSTM), or taxol-treated CTR cells (100 nmol/L). Cells were immunostained with PrlR (green), RAB7 (red), and nuclei (TO-PRO-3, blue). Scale bars, 18 μm. When not otherwise specified, $n = 3$ independent experiments were conducted.

breast cancer together and when dividing the analysis for each breast cancer subtype (Supplementary Fig. S5A–S5E).

Stathmin KO in Δ16HER2 transgenic mouse model leads to pronounced delay in mammary gland maturation and partial resistance to tumor formation

To verify the effect of stathmin ablation in breast cancer, we intercrossed STM KO mice with a transgenic mouse model of mammary tumorigenesis that expresses the Δ16HER2 oncogenic splicing variant in the mouse mammary gland (10). Δ16HER2 lacks 16 amino acids in the juxtamembrane domain, allowing this HER2 isoform to form stable and constitutively activated Δ16HER2 homodimers, with increased transforming potential compared with full-length HER2. The transgenic Δ16HER2 mouse develops multiple and multifocal mammary tumors already at 15 weeks of age, with a 100% penetrance (10).

Whole-mount analyses showed that, also in the context of Δ16HER2, STM KO virgin adult animals displayed a delayed development of the MMG (Supplementary Fig. S6A).

We analyzed neoplastic foci in 13-week-old Δ16HER2-positive animals, two weeks before the appearance of palpable tumors. As expected, these lesions were positive for HER2 expression, confirming that they were initiated by Δ16HER2 oncogenic expression, and were of the luminal subtype, because they expressed cytokeratin 8, but not cytokeratin 14 (Supplementary Fig. S6B and S6C). Intriguingly, these tumor foci displayed stathmin expression at much higher level than the surrounding normal mammary tissue, suggesting that stathmin expression might be a relevant step in Δ16HER2-driven tumor initiation (Fig. 6A). In line with the established role of stathmin as MT-destabilizer, level of acetylated-α-tubulin, marker of stable MTs, inversely correlates with that of stathmin, both in the MMG and in tumor foci (Fig. 6A).

We next focused on the evaluation of the impact of stathmin loss in the tumorigenic potential of Δ16HER2. At 13 weeks of age, the number of neoplastic lesions observed in Δ16HER2 mice was on average 4 foci/section of MMG, while Δ16HER2 STM KO mammary glands displayed almost no foci at this stage (Fig. 6B; $P = 0.0001$). Ki67 immunostaining of Δ16HER2 mammary glands showed that STM KO displayed a significant reduction in proliferating cell number, compared with WT ones (Fig. 6C; $P = 0.001$).

However, the decreased proliferation rate observed in the Δ16HER2 STM KO was not the cause of the reduced and/or delayed number of neoplastic lesions because, even at longer follow-up, these foci translated in significantly lower number of mammary tumors/mouse, as seen at 20 weeks of age (5 vs. 17 tumors/mice in STM KO vs. WT, Fig. 6D, $P = 0.007$). Also, these tumors displayed fewer Ki67-positive cells (Fig. 6E and F).

These findings support the possibility that stathmin loss renders mammary epithelial cells partially resistant to Δ16HER2-driven transformation.

Stathmin KO in Δ16HER2 transgenic mouse model reduces tumor growth by a cell-autonomous mechanism

Genetic ablation of stathmin in our model is not specific for mammary epithelial cells, so we could not rule out which component of the mammary gland was contributing the most to the observed phenotype. We thus performed syngeneic

Published OnlineFirst November 26, 2018; DOI: 10.1158/0008-5472.CAN-18-2488

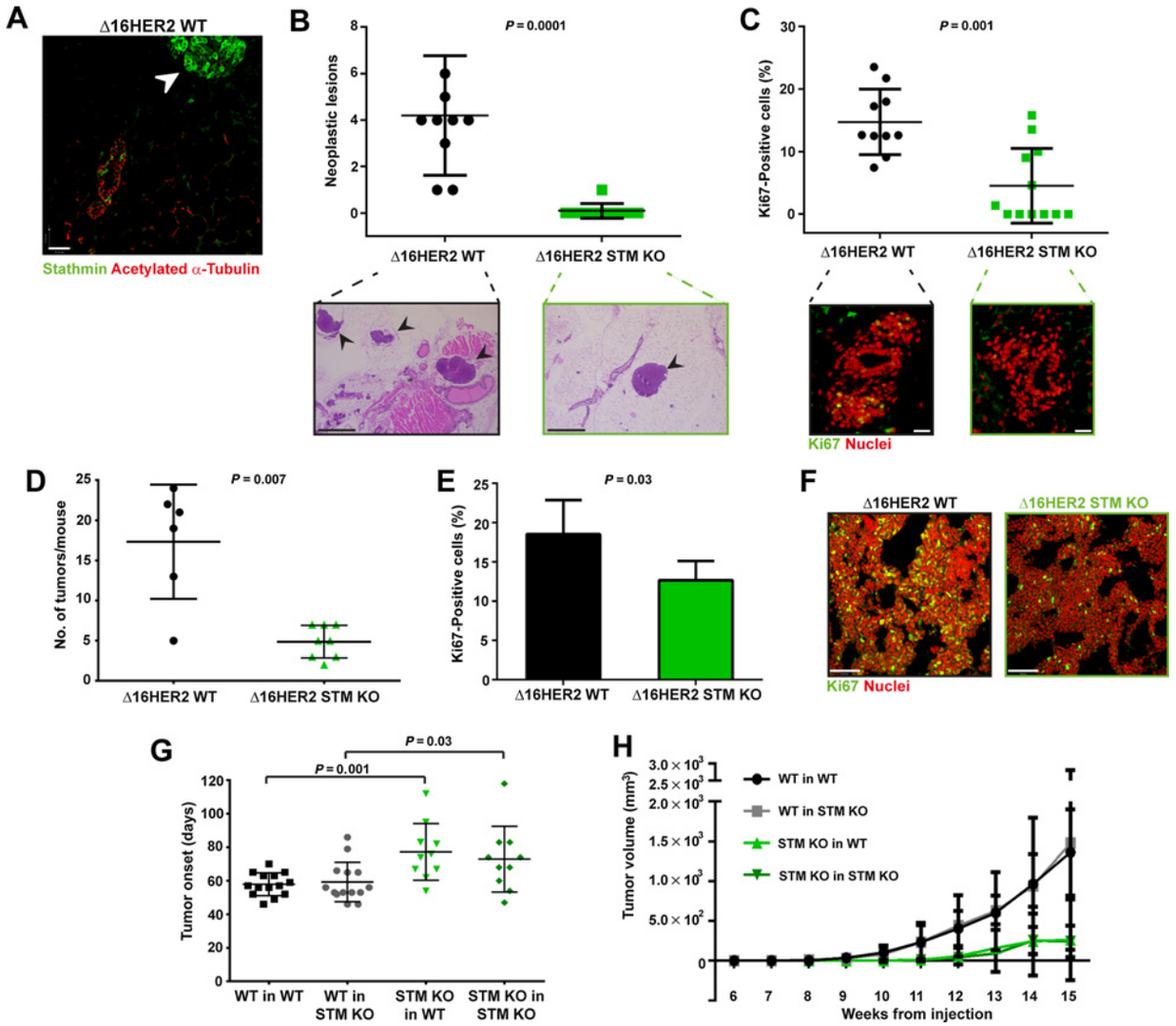

Figure 6.

Loss of stathmin induces partial resistance to Δ16HER2-driven tumorigenesis. **A,** Immunofluorescence analysis of stathmin (green) and acetylated α-tubulin (red) expression in MMG collected from Δ16HER2-WT mice at 13 weeks of age. Arrowhead, neoplastic lesion. Scale bars, 35 μm. **B,** Graph reports the number of neoplastic foci detected per hematoxylin and eosin–stained section of mammary glands collected from Δ16HER2-WT or -STM KO mice at 13 weeks of age, as indicated. Representative images of hematoxylin and eosin–stained mammary glands, taken with a 5× objective, are reported at the bottom of the graph. Arrowheads, neoplastic lesions. At least $n = 5$ mice/genotype were scored. Scale bars, 500 μm. **C,** Graph (top) and representative images (bottom) of Ki67-positive cells (green), evaluated by immunofluorescence analysis, in sections from the same samples described in **B**. Nuclei were stained with propidium iodide (red). Results are from $n = 5$ mice/genotype. Scale bars, 25 μm. **D,** Graph reports the number of tumors detected in Δ16HER2-positive, STM WT, or KO mice of 20 weeks of age (5–6 weeks from palpable tumor onset) at necropsy examination. At least 6 mice/group were evaluated. **E** and **F,** Graph (**E**) and representative images (**F**) of Ki67-positive cells (green), evaluated by immunofluorescence analysis in tumors from Δ16HER2-WT, or STM-KO mice described in **D**. Nuclei were stained with propidium iodide (red). Scale bars, 70 μm. **G** and **H,** Graphs report the onset (**G**) and growth (**H**) of palpable tumors derived from syngeneic injection experiments. Tumors from Δ16HER2-positive, WT-, or STM-KO mice (donors) were disaggregated and plated as primary cultures. Upon achievement of confluence, 3×10^5 cells were injected in mammary fat pad of Δ16HER2-negative, WT-, or STM-KO mice (recipients). At least 5 mice/group and three different cell populations/group were utilized. In all graphs, significance was calculated by Student t test or Mann–Whitney test, as appropriate, and is indicated by a $P < 0.05$.

injections experiments, to distinguish between the contributions of stathmin loss in transformed mammary epithelial cells (cell-autonomous role) from that in stromal cells (non–cell-autonomous role). Δ16HER2-transformed cells collected from tumors grown in Δ16HER2 STM WT or KO mice (donors) were implanted into nontransgenic WT or STM KO mice (recipients). The results clearly showed that Δ16HER2 STM KO tumor cells displayed longer latency (~ 80 vs 60 days) and their growth was slower, independently from the genotype of the recipient mouse (Fig. 6G and H).

Thus, stathmin expression in Δ16HER2-transformed mammary epithelial cells is important for tumor initiation and growth, while its expression or loss in stromal cells is not significantly involved in these processes.

Published OnlineFirst November 26, 2018; DOI: 10.1158/0008-5472.CAN-18-2488

Stathmin KO impairs the tumorigenic potential of Δ16HER2 mammary epithelial cells

On the basis of the phenotype observed in the normal mammary gland, we asked whether stathmin loss in Δ16HER2-transformed mammary epithelial cells impinged on the Prl/PrlR/STAT5 signaling pathway. However, STAT5 activation level was not different in the presence or absence of stathmin when Δ16HER2 tumors were analyzed (Fig. 7A). This result was somehow expected, because constitutive activation of HER2 signaling overrides the physiologic role of STAT5 signaling, as also demonstrated by others (35). We next looked at the mitotic spindle orientation in dividing mammary epithelial cells, in mice at 13 weeks of age, to evaluate whether this phenotype was conserved in the Δ16HER2 context. In line with what was observed in nontransgenic mice, Δ16HER2 STM KO mammary gland displayed a lower number of proliferating cells (Fig. 6C) and accumulated a substantial number of mitotic cells orienting their spindles with an angle greater than 30° with respect to the basement membrane (62%; Fig. 7B).

To better characterize this phenotype, we generated Δ16HER2-overexpressing NMuMG cells, silenced or not for stathmin (shSTM and CTR). When subjected to serum deprivation and then released to reenter into the cell cycle, Δ16HER2 NMuMG STM–silenced cells massively died (Fig. 7C), as also evidenced by the strong cleavage of caspase-3 (Fig. 7D). Accordingly, when challenged in clonogenic assay or in anchorage-independent cell growth, absence of stathmin led to significantly decreased number of colonies (Fig. 7E and F), further supporting that stathmin expression was necessary to sustain survival and tumorigenic potential of these cells. Together, these experiments strongly indicated that, in the context of Δ16HER2 oncogenic driver, stathmin was necessary to support the transformed phenotype of mammary epithelial cells.

To better characterize this point, we used a gene expression profiling approach looking at the coding genes in preneoplastic

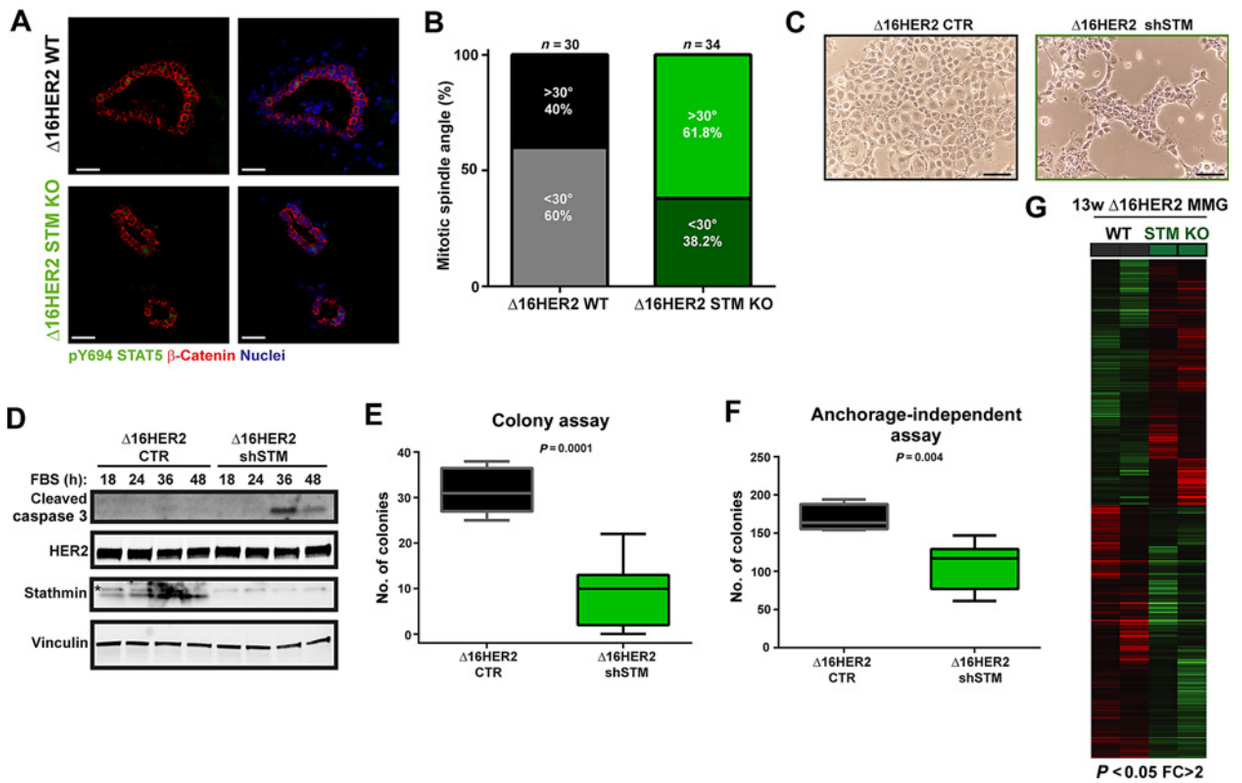

Figure 7.

Loss of stathmin in Δ16HER2 mammary epithelial cells leads to alteration of mitotic spindle orientation and decreased growth. **A,** Immunofluorescence analyses on sections from Δ16HER2-WT or -STM KO mammary tissue excised at 13 weeks of age, immunostained for pY694STAT5 (green), cytokeratin 8 (red), and nuclei (TO-PRO-3, blue). Images are representative of what observed in $n = 4$ different mice. Scale bars, 28 μm. **B,** Quantification of mitotic spindle angle in mammary glands from 13 weeks of age Δ16HER2-WT or -STM KO mice. The angle between mitotic axis and basement membrane was calculated using ImageJ in sections stained for pSer10-H3, α-tubulin, and nuclei. Results are from four mice/genotype. **C,** Pictures of NMuMG Δ16HER2-expressing cells transduced with Ad shCTR or Ad shSTM, serum starved, and released in complete medium for the indicated times. Pictures represent cells after 48 hours from release. Scale bars, 100 μm. **D,** Immunoblot analysis of lysates from cells described in **C**. Arrow, specific stathmin band. Asterisk, nonspecific band. Vinculin was used as loading control. **E,** Histogram displays the number of colonies formed by NMuMG clones expressing Δ16HER2 and stably silenced (shSTM) or not (CTR) for stathmin. Cells were stained with crystal violet and visible colonies were counted in $n = 3$ different clones tested. **F,** Anchorage-independent growth of NMuMG cells stably silenced (shSTM) or not (CTR) for stathmin. Cells were included in soft agar in presence of complete medium for 3 weeks. Graph reports the count of colony number from $n = 3$ different clones tested. When not otherwise specified, $n = 3$ independent experiments were conducted. When box whisker plots were used, minimum, median, and maximum values are shown in the graph. In all graphs, significance was calculated by Student t test or Mann–Whitney test, as appropriate, and is indicated by a $P < 0.05$. **G,** Heatmap showing the differential regulation of 502 probes ($P < 0.05$; FC>2) between MMG from 13 week-old Δ16HER2 mice, WT, or KO for stathmin gene.

Published OnlineFirst November 26, 2018; DOI: 10.1158/0008-5472.CAN-18-2488

mammary glands from 13-week-old WT and STM KO Δ16HER2 transgenic mice. Using a fold change (FC) cutoff >2 and a $P < 0.05$, we identified 502 genes differentially expressed between WT and STM KO (Fig. 7G). Interestingly, gene enrichment analyses demonstrated that STM absence dampened the expression of genes normally upregulated in HER2-preneoplastic signature and enriched those downregulated in HER2-preneoplastic signature, as defined by Landis (Supplementary Fig. S7A and S7B; Ref. 36), supporting a central role of STM for the establishment of HER2-driven transformation. Accordingly, STM KO Δ16HER2 preneoplastic mammary glands displayed lower expression of several oncogenic signatures, such as extracellular matrix remodeling and organization, luminal progenitors, TGFβ1 signaling, and breast cancer progression (Supplementary Fig. S7C–S7H).

Collectively, these data confirmed at molecular level that, before the establishment of an overt tumor phenotype, STM is necessary on one side to prevent mitotic defects that would eventually lead to cell apoptosis rather than tumor initiation, and, on the other hand, to establish a protumorigenic transcriptional program that leads to the formation of HER2-positive breast cancer in mice.

Discussion

Many processes implicated in mammary gland development are altered during breast cancer onset and progression, supporting the notion that understanding the mammary gland is critical to understanding breast cancer. Cell polarity is certainly one of these processes, fundamental in multicellular organisms for cell division, differentiation, organ morphogenesis, and disrupted in cancer (2). The establishment of cell polarity in the mammary gland involves a coordinated series of events, leading to asymmetric distribution of organelles and segregation of plasma membranes into an apical secretory domain, facing the lumen, and a basolateral one, in contact with the basement membrane (1). Microtubule organization contributes to the establishment of polarity at multiple levels. It is well known that, upon integrin-basement membrane engagement, microtubules polarize within the cell. The MT network polarization and its dynamics are then critical for determining oriented vesicle trafficking and segregation of components that establish unique cellular domains, eventually modeling the apicobasal polarity, orienting the mitotic spindle, and forming the mammary lumen structure (4, 5, 37, 38). In line with these notions, we show here that the MT-destabilizing protein stathmin governs processes strictly linked to polarity, such as trafficking, recycling of polarized proteins, and orientation of the mitotic spindle, necessary for MMG normal development. Our results indicate that loss of stathmin expression induces a marked delay in the postnatal maturation and development of normal mouse MMG, due to severe defects in the expansion and architecture of the epithelial cell compartment that eventually results in inability of female mice to nurse their litters. In particular, during pregnancy and lactation stages, stathmin loss led to decreased PrlR trafficking, stability, and intracellular signaling via STAT5. These data are in accord with previous demonstration that stathmin regulates the intracellular trafficking of IL4 receptor α in T lymphocytes (39) and Ras in fibroblasts (6).

We also observed that, after stathmin depletion, the mitotic spindle orientation of epithelial cells was randomized, with many spindles oriented in a way that they produce a daughter cell in the center of the lumen. This phenotype eventually resulted in mitotic aberrations and increased epithelial apoptosis, further contributing to disordered and delayed mammary gland organization. The first demonstration that impinging on microtubule dynamics could result in spindle misorientation came from Toyoshima and Nishida studies, showing that the activity of the microtubule stabilizing protein EB1 was necessary to orient the mitotic spindle of nonpolarized epithelial cells in 2D setting, *in vitro* (40). More recently, Akhtar and Streuli have demonstrated that Itgb1 KO mice display severely defective mammary gland morphogenesis due to disoriented epithelial cell polarity (5). At mechanistic level, they showed that absence of β1-integrin led to altered microtubule stabilization and polarization, eventually resulting in improper deposition of trafficking cargo along the apicobasal axis. Furthermore, the correct orientation of the mitotic spindle relies on binding to MTs of polarized protein, such as LGN and NuMA (37, 38). Thus, polarity controls the formation and maintenance of epithelial tissue architecture by ensuring the proper orientation of mitotic spindles during symmetric cell division.

We now add a new piece of information and show that the ablation of stathmin and the consequent disruption of MT dynamics, substantially alters all processes that require a functional cell polarity, from (dis)oriented mitosis to precise (de) localization of apicobasal markers, to eventual (de)formation of a (dis)organized ductal tree and development of a (im)mature MMG.

To what extent the downmodulation of the PrlR/STAT5 pathway observed in STM KO MMG is *per se* responsible for the morphogenic defects, has not been completely clarified by our experiments. However, considering the great impact that the altered mitotic spindle orientation played on mammary epithelial cell survival and on gland development, we believe that both processes contributed to the final phenotype of STM KO female mice.

We also evaluated the impact of stathmin loss in a mouse model of breast cancer, the MMTV-Δ16HER2 (10). Given the alteration of polarity and mitosis that we observed in the normal MMG, we quite expected to observe a promotion of the transformed phenotype, at least at late stages. On the contrary, all our data indicated that stathmin loss led to partial resistance to Δ16HER2-driven tumor formation. Although not obvious, our results are well in line with the pathologic evidence that stathmin is frequently hyper-, rather than hypoexpressed in breast cancer (8, 9, 34). Furthermore, high stathmin expression levels correlate with poor prognosis in patients with breast cancer (Supplementary Fig. S5). Our results are in line with those recently reported for Pik3c2a–null and Pten-null mouse mammary epithelial cells, in which misoriented cell division induces apoptosis as first *in vivo* effect, likely to preserve the mammary gland architecture and function (15, 29). However, while loss of PI3K-C2α initially impairs HER2/Neu tumor growth but later leads to the evolution of clones that exploit the presence of mitotic checkpoint defects (29), loss of luminal PTEN, as we observed here in the case of stathmin, is not sufficient for evading apoptosis and promoting tumor formation and progression (15).

Our molecular analyses on Δ16HER2-transformed cells demonstrated that stathmin loss strongly impacted on mitotic spindle disorientation, but no longer affected the Prl pathway. This result was somehow expected, for two main reasons. On one side, in the context of an overtly growing neoplastic lesion, the maintenance of polarity is lost by definition. On the other, it has been demonstrated that constitutive activation of HER2 signaling overrides

Published OnlineFirst November 26, 2018; DOI: 10.1158/0008-5472.CAN-18-2488

the functional role of Jak2/STAT5 signaling, particularly in the initial stages of mammary tumorigenesis (35). These data suggest that, in the context of Δ16HER2-established tumors, the intracellular pathway normally induced by Prl is already constitutively stimulated by the oncogenic transgene. However, we observed that stathmin expression was necessary to induce the complex transcriptional program associated with HER2 transformation, thus pointing to a central role in the context of both normal and transformed proliferating mammary epithelial cells.

Although our current data show that stathmin expression is critical for Δ16HER2-driven breast cancer onset, this finding cannot be generalized to all tumor contexts. We know already that following chemical carcinogenesis, relying on Ras or p53 mutations, stathmin is dispensable for tumor onset in mice, indicating that different pathways can overcome, solve, or even exploit the mitotic defects induced by stathmin loss, in different ways. Alternatively, because stathmin expression is generally low/undetectable in adult nonproliferating tissues, with the exception of brain, testis, and lymph nodes, it is also conceivable that its function could become only relevant in an organ, such as the developing mammary gland, in which stathmin expression is induced, as we observe during mouse pregnancy and lactation.

Our study has been performed both *in vitro*, in mouse and human models, and *in vivo*, in genetically modified mice. Beyond solid pathologic correlations, we need now to carefully verify the transferability of the new knowledge to the human pathology. In this regard, it is worth noting that taxanes, such as paclitaxel and docetaxel, whose mechanism of action is the inhibition of microtubule dynamics, are chemotherapeutic drugs that still represent a mainstay for treatment of breast cancer (but not only) patients. Future studies, establishing the implication of stathmin expression in the response to taxane-based therapies and, possibly, in the selection of taxane-responsive patients, may have important potential repercussion in the field of personalized cancer therapy.

Disclosure of Potential Conflicts of Interest

No potential conflicts of interest were disclosed.

Authors' Contributions

Conception and design: I. Segatto, A. Vecchione, G. Baldassarre, B. Belletti
Development of methodology: I. Segatto, M. De Marco Zompit, F. Citron, S. D'Andrea, G.L. Rampioni Vinciguerra, S. Berton, G. Mungo
Acquisition of data (provided animals, acquired and managed patients, provided facilities, etc.): G.L. Rampioni Vinciguerra, T. Perin, M. Schiappacassi, C. Marchini, A. Amici
Analysis and interpretation of data (e.g., statistical analysis, biostatistics, computational analysis): I. Segatto, M. De Marco Zompit, S. Berton, A. Vecchione, G. Baldassarre, B. Belletti
Writing, review, and/or revision of the manuscript: I. Segatto, G. Baldassarre, B. Belletti
Administrative, technical, or material support (i.e., reporting or organizing data, constructing databases): I. Segatto, B. Belletti
Study supervision: G. Baldassarre, B. Belletti

Acknowledgments

We would like to thank Dr. Paola Spessotto for support in confocal imaging, Dr. Riccardo Bomben for support in gene expression profiling, Mrs. Sara Benevol for technical assistance, past and present members of the S.C.I.C.C. lab for valuable contributions and all members of the Molecular Oncology Unit for critical discussion of the data. This work was supported by the Associazione Italiana Ricerca sul Cancro (AIRC; IG 16865 to G. Baldassarre) and (IG 20061 to B. Belletti); by CRO Intramural Research Grant (5 × 1000_2016_MdS to I. Segatto); by *L.R. 17*/2014-Regione FVG (TuMaGiDo to G. Baldassarre); by Associazione Italiana Ricerca sul Cancro (AIRC fellowships; #18171 to I. Segatto) and (#20902 to F. Citron).

The costs of publication of this article were defrayed in part by the payment of page charges. This article must therefore be hereby marked *advertisement* in accordance with 18 U.S.C. Section 1734 solely to indicate this fact.

Received August 9, 2018; revised October 17, 2018; accepted November 19, 2018; published first November 26, 2018.

References

1. Inman JL, Robertson C, Mott JD, Bissell MJ. Mammary gland development: cell fate specification, stem cells and the microenvironment. Development 2015;142:1028–42.
2. Visvader JE. Keeping abreast of the mammary epithelial hierarchy and breast tumorigenesis. Genes Dev 2009;23:2563–77.
3. Gadea BB, Ruderman JV. Aurora B is required for mitotic chromatin-induced phosphorylation of Op18/Stathmin. Proc Natl Acad Sci USA 2006;103:4493–8.
4. di Pietro F, Echard A, Morin X. Regulation of mitotic spindle orientation: an integrated view. EMBO Rep 2016;17:1106–30.
5. Akhtar N, Streuli CH. An integrin–ILK–microtubule network orients cell polarity and lumen formation in glandular epithelium. Nat Cell Biol 2013;15:17–27.
6. Fabris L, Berton S, Pellizzari I, Segatto I, D'Andrea S, Armenia J, et al. p27kip1 controls H-Ras/MAPK activation and cell cycle entry via modulation of MT stability. Proc Natl Acad Sci USA 2015;112:13916–21.
7. D'Andrea S, Berton S, Segatto I, Fabris L, Canzonieri V, Colombatti A, et al. Stathmin is dispensable for tumor onset in mice. PLoS One 2012;7:e45561.
8. Belletti B, Baldassarre G. Stathmin: a protein with many tasks. New biomarker and potential target in cancer. Expert Opin Ther Targets 2011;15:1249–66.
9. Curmi PA, Noguès C, Lachkar S, Carelle N, Gonthier MP, Sobel A, et al. Overexpression of stathmin in breast carcinomas points out to highly proliferative tumours. Br J Cancer 2000;82:142–50.
10. Marchini C, Gabrielli F, Iezzi M, Zenobi S, Montani M, Pietrella L, et al. The human splice variant Δ16HER2 induces rapid tumor onset in a reporter transgenic mouse. PLoS One 2011;6:e18727.
11. Debnath J, Muthuswamy SK, Brugge JS. Morphogenesis and oncogenesis of MCF-10A mammary epithelial acini grown in three-dimensional basement membrane cultures. Methods 2003;30:256–68.
12. Segatto I, Berton S, Sonego M, Massarut S, Fabris L, Armenia J, et al. p70S6 kinase mediates breast cancer cell survival in response to surgical wound fluid stimulation. Mol Oncol 2014;8:766–80.
13. Segatto I, Berton S, Sonego M, Massarut S, Perin T, Piccoli E, et al. Surgery-induced wound response promotes stem-like and tumor-initiating features of breast cancer cells, via STAT3 signaling. Oncotarget 2014;5:6267–79.
14. Belletti B, Vaidya JS, D'Andrea S, Entschladen F, Roncadin M, Lovat F, et al. Targeted intraoperative radiotherapy impairs the stimulation of breast cancer cell proliferation and invasion caused by surgical wounding. Clin Cancer Res 2008;14:1325–32.
15. Shore AN, Chang C-H, Kwon O-J, Weston MC, Zhang M, Xin L, et al. PTEN is required to maintain luminal epithelial homeostasis and integrity in the adult mammary gland. Dev Biol 2016;409:202–17.
16. Jaffe AB, Kaji N, Durgan J, Hall A. Cdc42 controls spindle orientation to position the apical surface during epithelial morphogenesis. J Cell Biol 2008;183:625–33.
17. Zheng Z, Zhu H, Wan Q, Liu J, Xiao Z, Siderovski DP, et al. LGN regulates mitotic spindle orientation during epithelial morphogenesis. J Cell Biol 2010;189:275–88.

18. Ince TA, Richardson AL, Bell GW, Saitoh M, Godar S, Karnoub AE, et al. Transformation of different human breast epithelial cell types leads to distinct tumor phenotypes. Cancer Cell 2007;12:160–70.
19. Bakin AV, Tomlinson AK, Bhowmick NA, Moses HL, Arteaga CL. Phosphatidylinositol 3-kinase function is required for transforming growth factor beta-mediated epithelial to mesenchymal transition and cell migration. J Biol Chem 2000;275:36803–10.
20. Belletti B, Nicoloso MS, Schiappacassi M, Berton S, Lovat F, Wolf K, et al. Stathmin activity influences sarcoma cell shape, motility, and metastatic potential. Mol Biol Cell 2008;19:2003–13.
21. Sonego M, Schiappacassi M, Lovisa S, Dall'Acqua A, Bagnoli M, Lovat F, et al. Stathmin regulates mutant p53 stability and transcriptional activity in ovarian cancer. EMBO Mol Med 2013;5:707–22.
22. Segatto I, Massarut S, Boyle R, Baldassarre G, Walker D, Belletti B. Preclinical validation of a novel compound targeting p70S6 kinase in breast cancer. Aging 2016;8:958–76.
23. Belletti B, Pellizzari I, Berton S, Fabris L, Wolf K, Lovat F, et al. p27kip1 controls cell morphology and motility by regulating microtubule-dependent lipid raft recycling. Mol Cell Biol 2010;30:2229–40.
24. Segatto I, Berton S, Sonego M, Massarut S, D'Andrea S, Perin T, et al. Inhibition of breast cancer local relapse by targeting p70S6 kinase activity. J Mol Cell Biol 2013;5:428–31.
25. Berton S, Pellizzari I, Fabris L, D'Andrea S, Segatto I, Canzonieri V, et al. Genetic characterization of p27kip1 and stathmin in controlling cell proliferation in vivo. Cell Cycle 2014;13:3100–11.
26. Schubart UK, Yu J, Amat JA, Wang Z, Hoffmann MK, Edelmann W. Normal development of mice lacking metablastin (P19), a phosphoprotein implicated in cell cycle regulation. J Biol Chem 1996;271:14062–6.
27. Mistry SJ, Atweh GF. Stathmin inhibition enhances okadaic acid-induced mitotic arrest: a potential role for stathmin in mitotic exit. J Biol Chem 2001;276:31209–15.
28. Villegas E, Kabotyanski EB, Shore AN, Creighton CJ, Westbrook TF, Rosen JM. Plk2 regulates mitotic spindle orientation and mammary gland development. Development 2014;141:1562–71.
29. Gulluni F, Martini M, De Santis MC, Campa CC, Ghigo A, Margaria JP, et al. Mitotic spindle assembly and genomic stability in breast cancer require PI3K-C2α scaffolding function. Cancer Cell 2017;32:444–459.e7.
30. Elias S, Thion MS, Yu H, Sousa CM, Lasgi C, Morin X, et al. Huntingtin regulates mammary stem cell division and differentiation. Stem Cell Rep 2014;2:491–506.
31. Ragkousi K, Gibson MC. Cell division and the maintenance of epithelial order. J Cell Biol 2014;207:181–8.
32. Ormandy CJ, Binart N, Kelly PA. Mammary gland development in prolactin receptor knockout mice. J Mammary Gland Biol Neoplasia 1997;2:355–64.
33. Kelly PA, Binart N, Lucas B, Bouchard B, Goffin V. Implications of multiple phenotypes observed in prolactin receptor knockout mice. Front Neuroendocrinol 2001;22:140–5.
34. Biaoxue R, Hua L, Wenlong G, Shuanying Y. Overexpression of stathmin promotes metastasis and growth of malignant solid tumors: a systemic review and meta-analysis. Oncotarget 2016;7:78994–9007.
35. Sakamoto K, Lin W, Triplett AA, Wagner K-U. Targeting Janus Kinase 2 in Her2/neu-Expressing mammary cancer: implications for cancer prevention and therapy. Cancer Res 2009;69:6642–50.
36. Landis MD, Seachrist DD, Montañez-Wiscovich ME, Danielpour D, Keri RA. Gene expression profiling of cancer progression reveals intrinsic regulation of transforming growth factor-beta signaling in ErbB2/Neu-induced tumors from transgenic mice. Oncogene 2005;24:5173–90.
37. Roignot J, Peng X, Mostov K. Polarity in mammalian epithelial morphogenesis. Cold Spring Harb Perspect Biol 2013;5:a013789. doi: 10.1101/cshperspect.a013789.
38. Knouse KA, Lopez KE, Bachofner M, Amon A. Chromosome segregation fidelity in epithelia requires tissue architecture. Cell 2018;175:200–11.
39. Tanaka Y, Hamano S, Gotoh K, Murata Y, Kunisaki Y, Nishikimi A, et al. T helper type 2 differentiation and intracellular trafficking of the interleukin 4 receptor-alpha subunit controlled by the Rac activator Dock2. Nat Immunol 2007;8:1067–75.
40. Toyoshima F, Nishida E. Integrin-mediated adhesion orients the spindle parallel to the substratum in an EB1- and myosin X-dependent manner. EMBO J 2007;26:1487–98.

Cancer Research
The Journal of Cancer Research (1916–1930) | The American Journal of Cancer (1931–1940)

AACR American Association for Cancer Research

Stathmin Is Required for Normal Mouse Mammary Gland Development and Δ16HER2-Driven Tumorigenesis

Ilenia Segatto, Mara De Marco Zompit, Francesca Citron, et al.

Cancer Res 2019;79:397-409. Published OnlineFirst November 26, 2018.